Volume 6 | Number 44 | 28 November 2015 | Pages 7633–7772

Polymer Chemistry

www.rsc.org/polymers

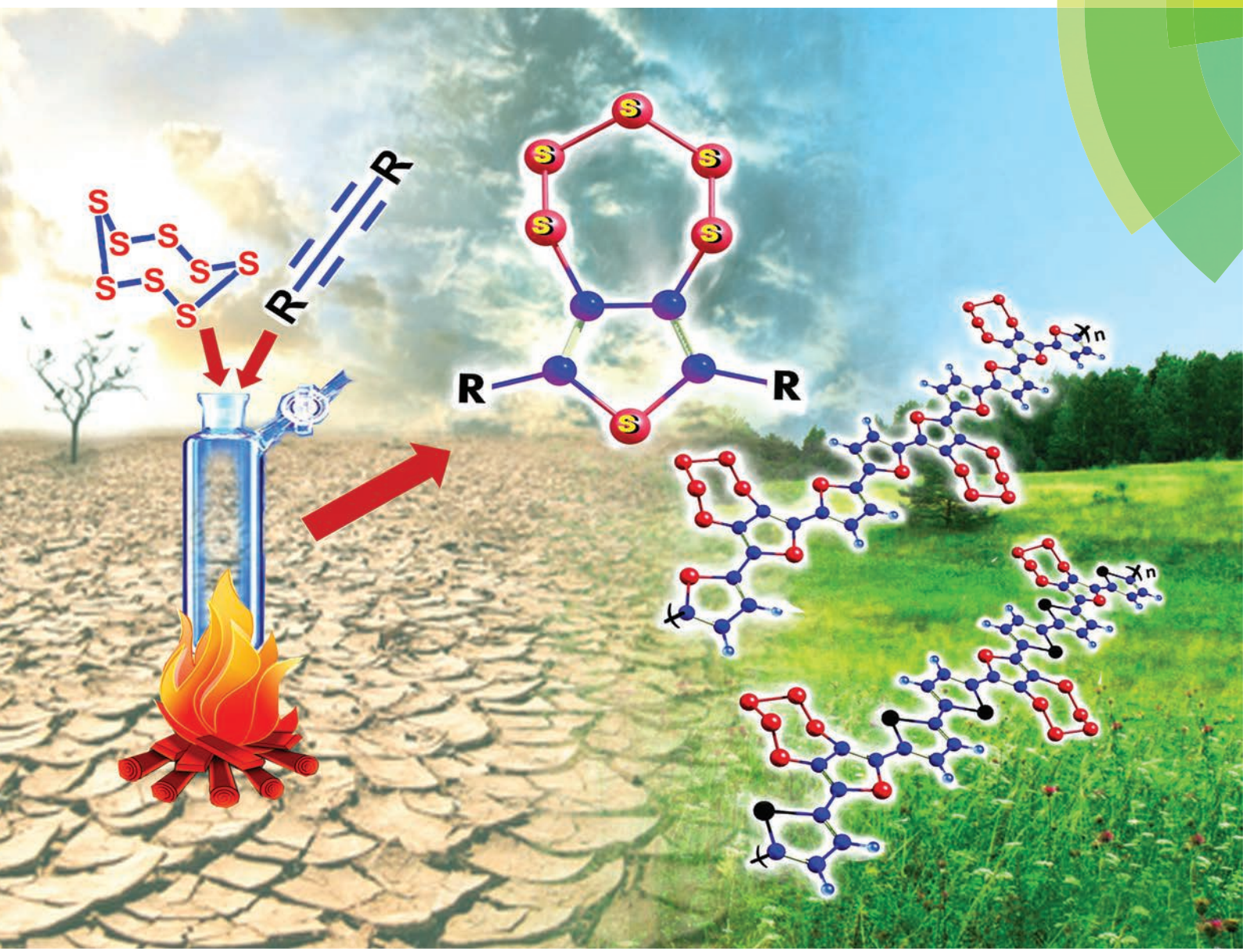

ISSN 1759-9954

ROYAL SOCIETY OF CHEMISTRY

PAPER

Sanjio S. Zade *et al.*

Thienopentathiepine: a sulfur containing fused heterocycle for conjugated systems and their electrochemical polymerization

Polymer Chemistry

PAPER

View Article Online
View Journal | View Issue

Cite this: *Polym. Chem.*, 2015, **6**, 7658

Thienopentathiepine: a sulfur containing fused heterocycle for conjugated systems and their electrochemical polymerization†

Sashi Debnath, Anjan Bedi and Sanjio S. Zade*

Received 20th July 2015,
Accepted 24th September 2015

DOI: 10.1039/c5py01133g

www.rsc.org/polymers

A series of conjugated building blocks based on the thieno[3,4-*f*][1,2,3,4,5]pentathiepine (C_4S_6) core has been synthesized by a new synthetic approach. The structural and optoelectronic properties of C_4S_6-derivatives are tuned by a judicious choice of end-capping. Chalcogenophene-capped derivatives (**2d**, **2e**, **2f**) were successfully electrochemically polymerized. The optical band gaps (E_g^{opt}) of **P1**, **P2** and **P3** were found to be in the range of 1.7–1.8 eV. A spectroelectrochemical study of the polymers showed reversibility in the formation of singly (polaron) and doubly charged (bipolaron) species.

Introduction

Thiophene-based conjugated systems represent one of the most widely investigated groups of π-conjugated materials[1,2] because of the potential industrial applications of these materials as active materials in organic electronic devices such as organic light-emitting diodes (OLEDs),[3] field-effect transistors (OFETs),[4,5] and photovoltaic cells (OPVs).[6,7] Structural modifications of the conjugated backbone are keystones to control the energy levels of the frontier orbitals and the optoelectronic properties of the resulting materials.[8] Developing a synthetic approach for new π-conjugated building blocks with the desired optoelectronic properties is imperative as conjugated materials with suitable consequences are limited.[9] Among the numerous chalcogenophene-based polymers, polythiophene (PT) derivatives have received growing attention because of their fundamental advantages such as (i) stronger donor characteristics, (ii) rigidity/crystallinity, (iii) good chemical stability, and (iv) high conductivity in the doped state.

Several strategies have been adopted to introduce new building blocks for conjugated materials with the desired properties. One of the important strategies includes synthesis of chalcogen containing heterocycles having multiple heteroatoms in the fused ring systems. An amplified spatial electronic arrangement because of the presence of multiple sulfur/selenium atoms in the molecular building blocks delocalizes the charge efficiently. In this regard, we have reported diselenolodiselenole (C_4Se_4) as a new building block for organic electronics, containing four selenium atoms in the central core.[10]

Chenard *et al.* reported the first synthesis of thieno[3,4-*f*]-[1,2,3,4,5]pentathiepine ($C_4H_2S_6$) in 2% yield where 3,4-dibromothiophene was used as a precursor.[11] In spite of the accessibility of the thienopentathiepine (C_4S_6) derivatives, synthetic reports are scant.[12–14] Although its nearest analogue benzopentathiepine has been explored to some extent its electrochemical properties were not investigated.[15–17] Recently, Swager and coworkers reported multiple sulfur containing fused dithiolodithiole (C_4S_4) derivatives focusing on their interesting structural and optoelectronic properties, where the formation of thienopentathiepines was observed as side products.[18] Here we report a new synthetic approach for the synthesis of thieno[3,4-*f*][1,2,3,4,5]pentathiepine derivatives as novel conjugated building blocks containing a fused pentathiepine ring in bicyclic heterocycles. Optoelectronic and structural properties were tuned by a judicial choice of end capping of the central C_4S_6 core. Chalcogenophene capped derivatives (**2d**, **2e**, **2f**) were electrochemically polymerized and the resulting polymers were successfully studied by spectroelectrochemistry.

Results and discussion

Synthesis of thieno[3,4-*f*][1,2,3,4,5]pentathiepine (C_4S_6) derivatives (**2a–2f**) involves heating of 1,4-disubstituted 1,3-butadiyne (**1a–1f**) with elemental sulfur near about the melting point of sulfur (125 °C) for 0.5 hour in a closed-flask

Department of Chemical Sciences, Indian Institute of Science Education and Research (IISER) Kolkata, Mohanpur, 741246, India.
E-mail: sanjiozade@iiserkol.ac.in

† Electronic supplementary information (ESI) available: ^{1}H and ^{13}C NMR spectra of all new compounds, crystallographic data and refinement parameters of single crystal X-ray structures, the ORTEP and packing diagram of **2a** and **2e**, spectroelectrochemistry of **P3**, TDDFT calculated molecular orbitals and excitations of **2d** and **2e**. CCDC 1049965, 1050201, 1050202 and 1050203. For ESI and crystallographic data in CIF or other electronic format see DOI: 10.1039/c5py01133g

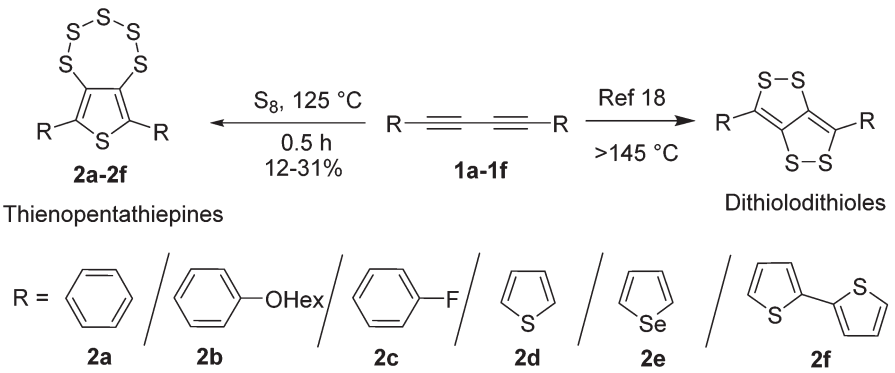

Scheme 1 Synthesis of C_4S_6 derivatives **2a–2f**.

(Scheme 1). Without using any initiator/catalyst, the yields were obtained in the range of 12–31%. This new synthetic approach is quick and simple compared to that of Chenard *et al.* and also benign in terms of precursors. The product yields did not improve by increasing the reaction time (up to 12 hours). In the presence of a solvent (1,2-dichloroethane) very low yields (2–3%) were obtained. The reaction at higher temperature (>150 °C) afforded C_4S_4 derivatives as previously reported by Swager *et al.*[18] The precursor diynes **1a–1f** were prepared either by a previously reported procedure[10,19,20] or by new synthetic strategies (see the ESI†). The conversion of diynes to C_4S_6 derivatives might proceed through the radical mechanism (Fig. S1†).[21]

Single crystal X-ray structures of 2a and 2c–2e

Crystals of **2a**, and **2c–2e** suitable for single crystal X-ray crystallography were obtained from slow evaporation of their dichloromethane solutions. In the molecular structure of **2a**, terminal phenyl rings are twisted from the central thiophene core by dihedral angles of ~37° and ~45° (Fig. S2a†), whereas the packing diagram shows formation of 1D chains *via* intermolecular interactions (S3–C8 = 3.40 Å and S4–S6 = 3.47 Å) (Fig. S2c†). Similarly in the molecular structure of **2c** (Fig. S2b†), both *p*-fluoro substituted phenyl rings are twisted by a dihedral angle of ~43° from the central thiophene of the C_4S_6-core. The structure of **2c** exhibits resolute S···S intermolecular interaction (S4–S3 = 3.39 Å and S4–S5 = 3.39 Å). In the structures **2a** and **2c**, the S···S interaction leads to the arrangement of a virtual –(S–S···S–S)$_n$– polymeric chain along the *b*- and *a*-axes, respectively (Fig. S2c and S2d†).

In the molecular structure of **2d** and **2e**, the terminal thiophene and selenophene rings are *anti* to the central thiophenes (Fig. 1).[22] In the thiophene-capped C_4S_6-derivative **2d**, the torsional angles of the terminal thiophenes with the central thiophene of the C_4S_6-core are ~9° and ~23°, respectively; whereas in the selenophene-capped C_4S_6-derivative **2e**, the corresponding torsional angles are ~3° and ~7°. It is congruent with the earlier reports[23,24] which showed that selenophene based conjugated systems are more planar and rigid because of the low aromaticity of selenophene and the higher polarizability of Se. In the crystal packing of **2d**, three molecules are connected by four S···S interactions (S1–S8 = 3.56 Å (two), S6–S6 = 3.48 Å, and S3–S7 = 3.47 Å) (Fig. 1b) to form a 2D zip-lock structure.[25,26] In compound **2e**, Se···C (Se2–C10 = 3.55 Å (forming π-stacking dimer) and Se2–C11 = 3.59 Å) and S···S (S5–S6 = 3.43 Å) interactions form a typically 2D closed packed arrangement (Fig. 1d). In **2e**, the S···S interaction constructs a –(S–S···S–S)$_n$– polymeric chain.

Optical and electrochemical properties of 2a–2f

Compounds **2a–2f** exhibited two distinct absorption bands in their absorption spectra with absorption maxima (λ_{max}) ranging from 258 to 277 nm (high energy bands) and 316 to 429 nm (relatively broad and low energy bands) (Fig. 2a). TD-DFT calculations on **2d** and **2e** indicate that the lower energy absorption bands include (i) the π → π* (HOMO → LUMO) transition of the terthiophene/selenophene–thiophene–selenophene backbone and (ii) the transition from the π-orbital of terthiophene/selenophene–thiophene–selenophene to the π* orbital of the central thiophene ring coupled with the antibonding orbitals of S–S bonds of the pentathiepine heterocycle (Tables S2 and S3†). The higher energy band mainly originates from (i) the transition from the π orbital (HOMO) to the antibonding orbitals of the pentathiepine heterocycle and (ii) the non-bonding orbital on the S atoms of pentathiepine to the π* orbital (LUMO). Compounds with electron donating groups exhibited a bathochromic shift in the absorption spectra. The absorption spectrum of selenophene-capped **2e** showed a red shift (of 27 nm) compared to that of thiophene-capped **2d** because of the better conjugation in **2e**. The bithiophene-capped C_4S_6-derivative **2f** showed lower-energy absorption bands due to the extended conjugation.

Cyclic voltammograms (CV) of **2a–2f** showed irreversible oxidation peaks ranging from 0.80 V to 1.60 V *vs.* Ag/AgCl (Fig. 2b).[27] Although selenophene is electron rich compared to thiophene, **2e** exhibited higher oxidation potential than **2d**. The planar conjugated backbone of **2e** could result in superior delocalization of the electrons throughout the molecular plane, which might decrease the electron density on the C_4S_6

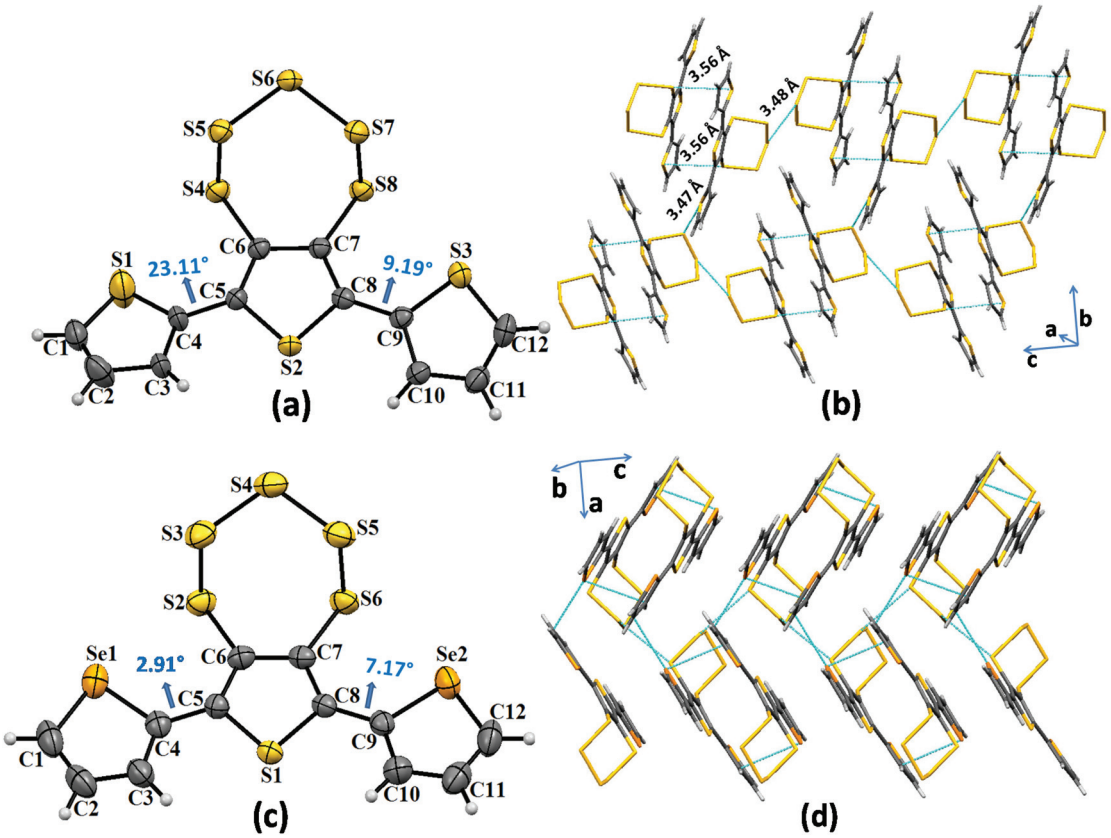

Fig. 1 (a) and (c) ORTEP diagram of **2d** and **2e**, (b) and (d) packing of **2d** and **2e**. The ellipsoids are drawn at the 50% probability level in (a) and (c).

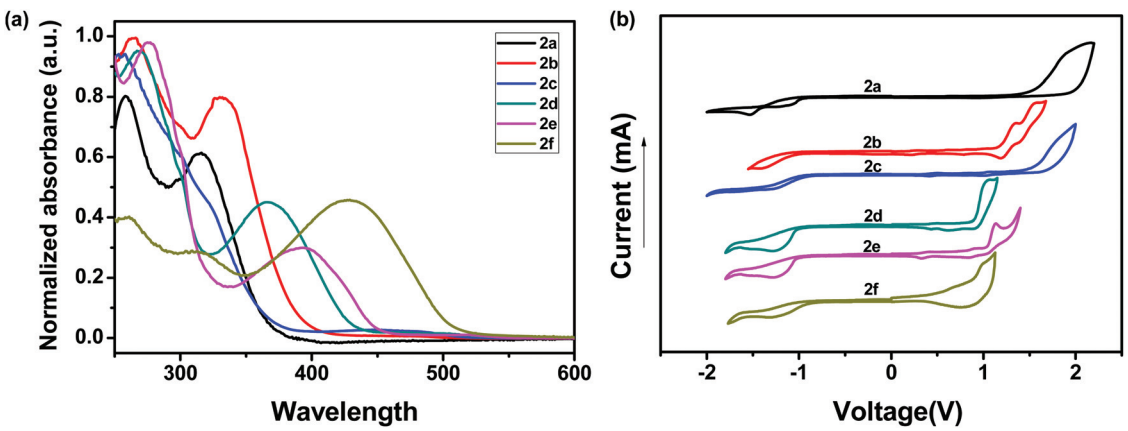

Fig. 2 (a) UV-vis spectra in DCM and (b) electrochemical properties of compounds **2a–2f** in 0.1 M $TBAPF_6$ in dry DCM as the solvent using a Pt-disk working electrode, a Pt-wire counter electrode and a Ag/AgCl reference electrode.

unit. The UV-vis and CV data were used to measure the band gap (E_g) and HOMO/LUMO energy levels (Table 1).

Electrochemical properties of the polymers

Under repeated CV cycles, compounds **2d**, **2e** and **2f** polymerized smoothly *via* progressive growth of a visible polymer film a platinum-disk working electrode (Scheme 2, Fig. 3, and S3†). The polymer films were investigated for their scan rate dependence at 50–250 mV s^{-1} for **P1** and 50–300 mV s^{-1} for **P2** and **P3**. All the polymers showed linear scaling of the anodic currents with the increasing value of scan rate (Fig. 3c, d and S3†), as expected from an electrode-supported electroactive

Table 1 Yields, absorption and electrochemical properties of **2a–2f**

Compounds	% Yield	λ_{max}(nm)	E^{ox}_{onset}(V)	$E_g^{opt\,a}$ (eV)	E_{HOMO} [b](eV)	E_{LUMO} [c](eV)
2a	27	258, 316	1.53	3.40	−5.97	−2.57
2b	31	266, 330	1.14	3.22	−5.58	−2.36
2c	22	258	1.49	3.41	−5.93	−2.52
2d	17	270, 366	0.90	2.87	−5.34	−2.47
2e	12	277, 393	1.01	2.73	−5.44	−2.71
2f	21	261, 429	0.76	2.45	−5.20	−2.75

[a] $E_g^{opt} = 1240/\lambda_{onset}$. [b] $E_{HOMO} = -4.44 + E^{ox}_{onset}$. [c] $E_{LUMO} = E_{HOMO} + E_g^{opt}$.

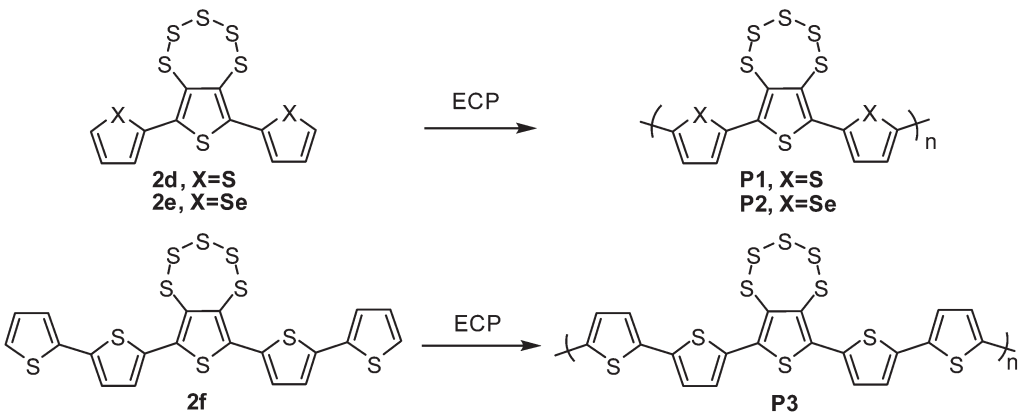

Scheme 2 Synthesis of polymers **P1**, **P2** and **P3**.

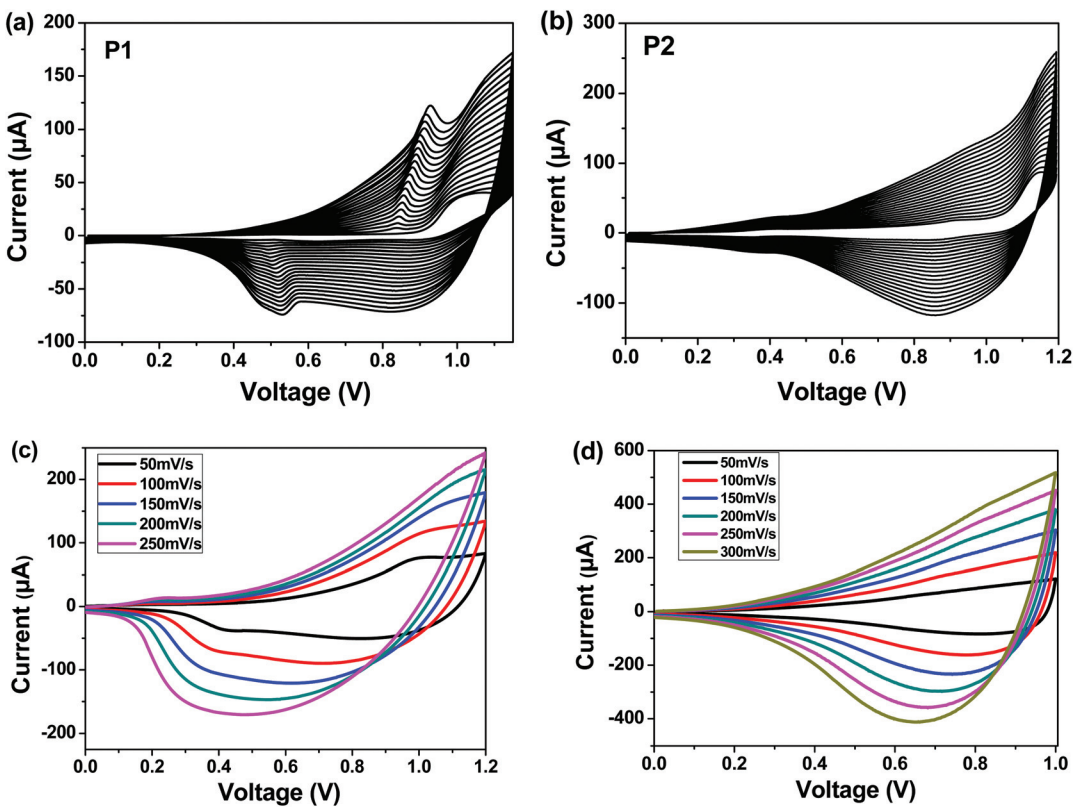

Fig. 3 (a) and (b) Multisweep electropolymerization of **2d** and **2e** on a Pt electrode in DCM and 0.1 M $TBAPF_6$ at 50 mV s^{-1} *vs.* Ag/AgCl wire. (c) and (d) CV of **P1** and **P2** in monomer free DCM and 0.1 M $TBAPF_6$ as a function of scan rate.

film. Cyclic voltammograms of **P1**, **P2**, and **P3** polymer films on a Pt working electrode showed quasi-reversible p-doping/dedoping processes over a positive potential range in the DCM/0.1 M $TBAPF_6$ solvent/electrolyte system at 50 mV s^{-1} scan rate (Fig. 4b). The onsets of the oxidation potentials (E^{ox}_{onset}) of **P1**, **P2** and **P3** were found to be 0.67, 0.49 and 0.43 V, respectively, corresponding to the HOMO levels at −5.11, −4.93 and−4.87 eV, respectively. The LUMO levels, estimated from the HOMO and the onsets of the absorption peaks, were found to be −3.35, −3.27, and−3.07 eV for **P1**, **P2**, and **P3**, respectively (Fig. 4, Table 2). **P2** exhibited a lower oxidation potential than **P1**, which can be attributed to the presence of more polarizable Se.

Spectroelectrochemistry

Polymers were chronoamperometrically deposited on an ITO-coated glass electrode from 1×10^{-2} M monomer solutions in DCM and the spectroelectrochemical properties were investigated *in situ* in the monomer-free electrolyte solution under a variety of voltage pulses. The absorption spectra in the UV–vis–NIR region of **P1**, **P2** and **P3** films (Fig. 5, S4†) revealed good electrochromic nature at distinct applied potentials in the DCM/$TBAPF_6$ solvent/electrolyte couple. The onset values of the lowest energy bands correspond to the optical band gaps (E^{opt}_g) of 1.76, 1.69 and 1.80 eV for **P1**, **P2** and **P3**, respectively (Table 2). **P2** exhibited a smaller band gap than **P1** because of

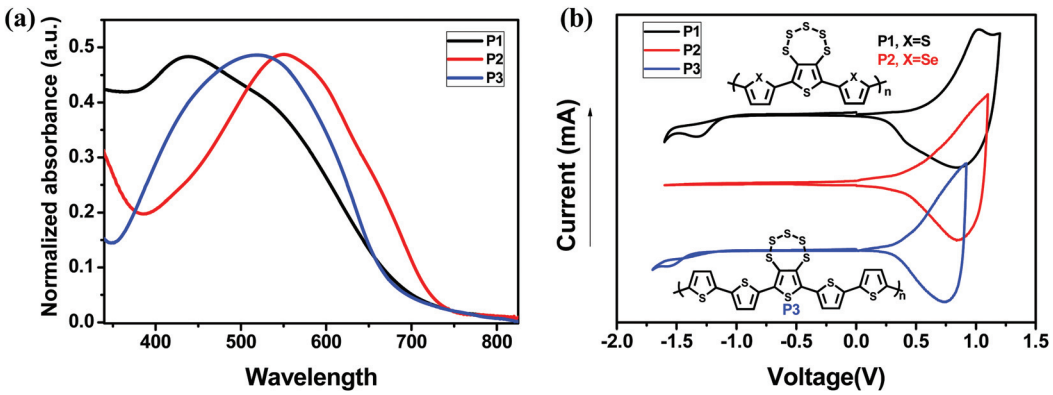

Fig. 4 (a) Absorption spectra of **P1**–**P3** in thin film. (b) CV of **P1**, **P2** and **P3**, using the DCM/$TBAPF_6$ solvent/electrolyte system.

Table 2 Absorption and electrochemical properties of **P1**, **P2** and **P3**

Polymer	λ_{max}(nm)	E^{opt}_g (eV)	E^{ox}_{onset}(V)	E_{HOMO} (eV)	E_{LUMO} (eV)
P1	439	1.76	0.67	−5.11	−3.35
P2	550	1.69	0.49	−4.93	−3.27
P3	518	1.80	0.43	−4.87	−3.07

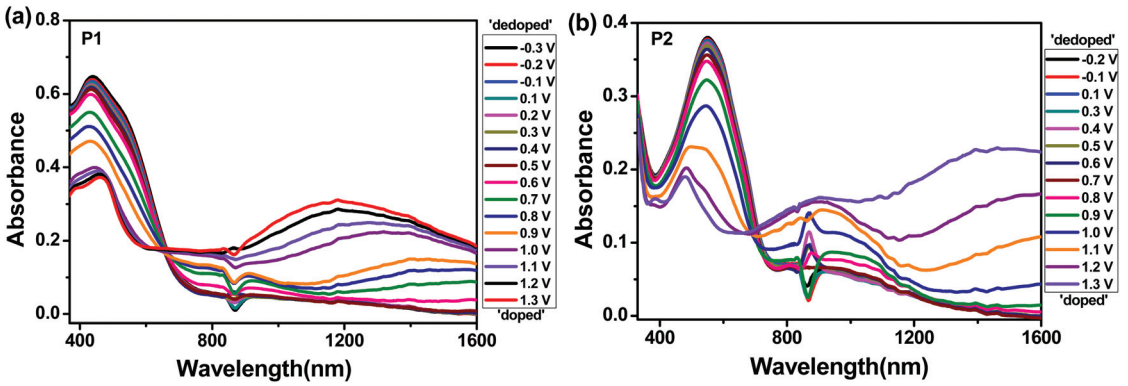

Fig. 5 Spectroelectrochemistry of (a) **P1** and (b) **P2** thin films prepared on ITO-coated glass as a function of applied potential between −0.3 and +1.3 V for **P1**, and −0.2 and +1.3 V for **P2** in DCM.

the presence of selenophene in **P2** instead of thiophene in **P1**. Notably, these polymers having the fused pentathiepine ring as a substituent on thiophene possess a smaller band gap compared to polythiophene (2.0 eV) and polyselenophene (1.9 eV).[2,28,29] The band gaps of all three polymers remained in between the band gaps of poly(3-hexylthiophene) (1.9 eV) and poly(3-hexylselenophene) (1.6 eV).[30,31] The lowering in the band gap of these polymers can be attributed to the delocalization of the π electron density over the pentathiepine rings and interchain interactions due to the presence of multiple sulphur atoms.

In the spectroelectrochemical experiments, switching of the polymers from neutral to oxidized states was associated with the color change from deep brown to transparent-peach for **P1**, purple to transparent-gray for **P2**, and violet to transparent-gray for **P3**. With the increasing applied potential, the intensity of the absorption band in the visible region (arises due to the π–π* transition) was gradually decreased and two new bands gradually appeared in the higher wavelength region. New peaks at 820, 905, and 750 nm for **P1**, **P2** and **P3**, respectively, in their absorption spectra (Fig. 5 and S4†) indicate the formation of singly charged species (polaron), while the lower energy bands at 1180, 1480, and 1160 nm correspond to the formation of doubly charged species (bipolaron), respectively.[32,33] The deviation in spectroelectrochemical experiments precisely comes at 850 nm (Fig. 5a and b) which is due to the lamp change (deuterium to tungsten lamp) during the NIR region to VIS region transformation.

Conclusion

In conclusion, a series of conjugated compounds, thieno[3,4-*f*][1,2,3,4,5]pentathiepine derivatives, was synthesized by a simple synthetic method of heating diaryl diynes with elemental sulfur. The structural and optoelectronic properties of C_4S_6-derivatives were tuned successfully by the choice of end capping. Multiple close S···S contacts due to the presence of a fused pentathiepine ring in C_4S_6-derivatives and their polymers may be beneficial for the extended conjugation and charge transport. The C_4S_6-derivatives with thiophene- and selenophene-capping were successfully electrochemically polymerized. The low band gap polymers **P1–P3** exhibited well-defined spectroelectrochemistry and sufficient stability in the oxidized state, which can be exploited for organic electronic devices.

Experimental section

Most of the reagents and solvents of reagent grade were obtained from commercial sources and used without any further purification. NMR spectra were recorded on a Jeol-ECS 400 MHz spectrometer using $CDCl_3$/C_6D_6 as the solvent and chemical shifts are reported in parts per million (δ scale) relative to tetramethylsilane (TMS) as the internal standard. Columns were equipped with silica gel (100–200 mesh). A non-aqueous Ag/AgCl electrode was made by dipping silver wire into a $FeCl_3$/HCl solution. Electrochemical analysis was carried out with a Princeton Applied Research 263A potentiostat using a platinum (Pt) disk electrode (dia. 1.6 mm) as the working electrode, a platinum wire as the counter electrode, and an AgCl coated Ag wire as the reference electrode. Pt disk electrodes were gleamed with alumina, water, and acetone and were dried with nitrogen to remove any incipient oxygen. The electrolyte used was 0.1 M $TBAPF_6$ in DCM. Films were electrodeposited in 0.1 M $TBAPF_6$ in DCM by cyclic voltammetry (CV) between various applied potentials at 50 mV s^{-1} for 20 cycles. **2d**, **2e** and **2f** were electrochemically polymerized on indium tin oxide (ITO) coated glass as a working electrode. Before examining the optical properties of polymer films, the films were rinsed with DCM. UV-vis-NIR spectra were recorded on a HITACHI U-4100 UV-vis-NIR spectrophotometer.

Fine crystals of **2a** and **2c–2e** were collected on a SuperNova, Dual, Cu/Mo at zero, Eos diffractometer. Using Olex2,[34] the structure was solved with the Superflip[35] structure solution programme applying Charge Flipping and refined with the ShelXL[36] refinement package applying least squares minimization.

Synthesis of 1e

A tetrabutylammonium fluoride solution (3 mL, 1 M in THF) was added dropwise into a stirred solution of trimethyl(selenophen-2-ylethynyl)silane (500 mg, 2.19 mmol) in 10 mL THF and stirred for 10 min at rt. This solution was added into a three necked round-bottom flask containing $Cu(OAc)_2$ (553 mg, 3.06 mmol) and 10 mL of pyridine/methanol mixture (1 : 1 v/v) and refluxed for 2 h. The reaction mixture was allowed to cool at rt and added to crushed-ice and 3.6 mL of 9 M H_2SO_4. The resulting solution was extracted with diethyl ether (3 × 25 mL). The ether layers were mixed, dried over anhydrous Na_2SO_4 and concentrated to produce a deep brown crude product. Column chromatography of the crude on silica gel using hexane as the eluent gave **1e** as a pale yellow solid (170 mg, 50%). ^{1}H NMR (400 MHz, δ, ppm, $CDCl_3$): 8.07 (d, 2H, *J* = 4.6 Hz), 7.54 (d, 2H, *J* = 3.44 Hz), 7.24–7.21 (m, 2H,). ^{13}C NMR (100 MHz, $CDCl_3$): δ 136.6, 134.9, 129.6, 126.0, 79.6, 79.5.

Synthesis of 1f

Compound **1f** was synthesized by using a similar synthetic procedure to **1e** using (2,2′-bithiophen-5-ylethynyl)trimethylsilane (563 mg, 2.15 mmol), which afforded **1f** as a pale brown solid (300 mg, 73%). ^{1}H NMR (400 MHz, δ, ppm, C_6D_6): 6.83 (d, 2H, *J* = 3.84 Hz), 6.80 (d, 2H, *J* = 3.84 Hz), 6.65 (d, 2H, *J* = 5.36 Hz), 6.57–6.52 (m, 4H). ^{13}C NMR (100 MHz, C_6D_6): δ 140.9, 136.5, 135.8, 128.1, 125.5, 125.0, 123.8, 120.6, 79.8, 78.1.

General procedure for the synthesis of 2a–2f

Butadienes (1 mmol) and sulfur powder (8 mmol) were charged into a Schlenk flask and it was stoppered. The reaction mixture was heated at 125 °C for 0.5 h. The reaction was cooled and the resulting residue was purified by column chromatography on 100–200 mesh silica gel (2% CH_2Cl_2 in hexane) to obtain the products.

2a: Yellowish brown solid. Yield: 106 mg, 27%. M.p.: 154 °C. UV-vis in DCM: λ_{max} (nm) ($10^4 \times \varepsilon$ (M^{-1} cm^{-1})) = 258 (4.5), 316 (3.4). ^{1}H NMR (400 MHz, $CDCl_3$): δ 7.55–7.51 (m, 2H), 7.49–7.43 (m, 3H). ^{13}C NMR (100 MHz, $CDCl_3$): δ 148.3, 137.9, 132.5, 130.0, 129.1, 128.5. HRMS (ESI+): calculated for $C_{16}H_{10}S_6$, 393.9107; found 393.9029.

2b: Yellow solid. Yield: 184 mg, 31%. M.p.: 122 °C. UV-vis in DCM: λ_{max} (nm) ($10^4 \times \varepsilon$ (M^{-1} cm^{-1})) = 266 (5.9), 330 (4.7). ^{1}H NMR (400 MHz, $CDCl_3$): δ 7.46 (d, 2H, J = 8.4 Hz), 6.97 (d, 2H, J = 8.4 Hz), 4.00 (t, 2H), 1.80 (m, 2H), 1.51–1.43 (m, 2H), 1.38–1.32 (m, 4H), 0.91 (t, 3H). ^{13}C NMR (100 MHz, $CDCl_3$): δ 159.9, 147.9, 136.8, 131.2, 124.7, 114.4, 68.1, 31.5, 29.1, 25.7, 22.5, 14.0. HRMS (ESI+): calculated for $C_{28}H_{34}O_2S_6$, 594.0883; found 594.0229.

2c: Yield: 94 mg, 22%. M.p.: 143 °C. UV-vis in DCM: λ_{max} (nm) ($10^{-4} \times \varepsilon$ (M^{-1} cm^{-1})) = 258 (7.8). ^{1}H NMR (400 MHz, $CDCl_3$): δ 7.53–7.48 (m, 2H), 7.19–7.13 (m, 2H). ^{13}C NMR (100 MHz, $CDCl_3$): δ 164.2 (d, J = 199.3 Hz), 138.1, 134.5 (d, J = 6.5 Hz), 131.9 (d, J = 6.5 Hz), 128.5, 115.8 (d, J = 18.05 Hz). HRMS (ESI+): calculated for $C_{16}H_8F_2S_6$, 429.8918; found 429.8120.

2d: Yellowish brown solid. Yield: 68 mg, 17%. M.p.: 167 °C. UV-vis in DCM: λ_{max} (nm) ($10^{-4} \times \varepsilon$ (M^{-1} cm^{-1})) = 270 (9.5), 366 (4.4). ^{1}H NMR (400 MHz, $CDCl_3$): δ 7.45 (d, 2H, J = 3.80 Hz), 7.40 (d, 2H, J = 3.84 Hz), 7.18–7.07 (m, 2H). ^{13}C NMR (100 MHz, $CDCl_3$): δ 140.5, 136.7, 133.8, 128.5, 128.4, 127.3. HRMS (ESI+): calculated for $C_{12}H_6S_8$, 405.8235; found 404.8191.

2e: Yellowish brown solid. Yield: 60 mg, 12%. M.p.: 179 °C. UV-vis in DCM: λ_{max} (nm) ($10^{-4} \times \varepsilon$ (M^{-1} cm^{-1})) = 277 (10.5), 393 (3.2). ^{1}H NMR (400 MHz, $CDCl_3$): δ 8.16 (d, 2H, J = 5.32 Hz), 7.61 (d, 2H, J = 3.8 Hz), 7.34–7.30 (m, 2H). ^{13}C NMR (100 MHz, $CDCl_3$): δ 142.4, 138.0, 136.3, 134.9, 130.2, 129.4. HRMS (ESI+): calculated for $C_{12}H_6S_6Se_2$, 501.7124; found 501.7051.

2f: Deep orange solid. Yield: 118 mg, 21%. M.p.: 194 °C. UV-vis in DCM: λ_{max} (nm) ($10^{-4} \times \varepsilon$ (M^{-1} cm^{-1})) = 261 (4.0), 429 (4.5). ^{1}H NMR (400 MHz, C_6D_6): δ 6.96–6.92 (m, 4H), 6.81 (d, 2H, J = 3.8 Hz), 6.70 (d, 2H, J = 3.84 Hz), 6.61 (m, 2H). ^{13}C NMR (100 MHz, C_6D_6): δ 150.4, 148.4, 147.2, 143.4, 139.3, 139.2, 127.3, 124.8, 124.3, 120.0. HRMS (ESI+): calculated for $C_{20}H_{10}S_{10}$, 569.7990; found 569.8073.

Theoretical methods

Single point TD-DFT calculations were performed on the structure obtained from the single crystal X-ray diffraction of **2d** and **2e** by using the Gaussian 09 programme[37] at the B3LYP/6-31G(d) level.

Acknowledgements

We thank DST, India for funding. SD thanks UGC and AB thanks CSIR for a research fellowship.

References

1 W. Ni, X. Wan, M. Li, Y. Wang and Y. Chen, *Chem. Commun.*, 2015, **51**, 4936.
2 *Handbook of Thiophene-Based Materials*, ed. I. F. Perepichka and D. F. Perepichka, Wiley-VCH, Chichester, UK, 2009.
3 P. Furuta, J. Brooks, M. E. Thompson and J. M. J. Fréchet, *J. Am. Chem. Soc.*, 2003, **125**, 13165.
4 C. Wang, H. Dong, W. Hu, Y. Liu and D. Zhu, *Chem. Rev.*, 2012, **112**, 2208.
5 Y. S. Yang, T. Yasuda, H. Kakizoe, H. Mieno, H. Kino, Y. Tateyama and C. Adachi, *Chem. Commun.*, 2013, **49**, 6483.
6 P. M. Beaujuge and J. M. J. Fréchet, *J. Am. Chem. Soc.*, 2011, **133**, 20009.
7 K. Feng, X. Xu, Z. Li, Y. Li, K. Li, T. Yu and Q. Peng, *Chem. Commun.*, 2015, **51**, 6290.
8 Y. Liang, D. Feng, Y. Wu, S. T. Tsai, G. Li, C. Ray and L. Yu, *J. Am. Chem. Soc.*, 2009, **131**, 7792.
9 X. He, J. Borau-Garcia, A. Y. Y. Woo, S. Trudel and T. Baumgartner, *J. Am. Chem. Soc.*, 2013, **135**, 1137.
10 A. Bedi, S. Debnath and S. S. Zade, *Chem. Commun.*, 2014, **50**, 13454.
11 B. L. Chenard, R. L. Harlow, A. L. Johnson and S. A. Vladuchick, *J. Am. Chem. Soc.*, 1985, **107**, 3871.
12 L. S. Konstantinova, O. A. Rakitin, C. W. Rees, L. I. Souvorova, D. G. Golovanov and K. A. Lyssenko, *Org. Lett.*, 2003, **5**, 1939.
13 S. A. Amelichev, L. S. Konstantinova, O. A. Rakitin and C. W. Rees, *Mendeleev Commun.*, 2006, **16**, 289.
14 M. J. Earle, A. G. Massey, A.-R. AL-Soudani and T. Zaidi, *Polyhedron*, 1989, **8**, 2817.
15 B. L. Chenard and T. J. Miller, *J. Org. Chem.*, 1984, **49**, 1221.
16 D. Aebisher, E. M. Brzostowska, N. Sawwan, R. Ovalle and A. Greer, *J. Nat. Prod.*, 2007, **70**, 1492.
17 E. M. Brzostowska and A. Greer, *J. Org. Chem.*, 2004, **69**, 5483.
18 D. J. Schipper, L. C. H. Moh, P. Müller and T. M. Swager, *Angew. Chem., Int. Ed.*, 2014, **53**, 5847.
19 I. D. Campbell and G. Eglinton, *Org. Synth.*, 1965, **45**, 39.
20 Y. Arakawa, S. Nakajima, R. Ishige, M. Uchimura, S. Kang, G.-i. Konishi and J. Watanabe, *J. Mater. Chem.*, 2012, **22**, 8394.
21 G. Zhang, H. Yi, H. Chen, C. Bian, C. Liu and A. Lei, *Org. Lett.*, 2014, **16**, 6156.
22 M. D. Curtis, J. Cao and J. W. Kampf, *J. Am. Chem. Soc.*, 2004, **126**, 4318.
23 Y. H. Wijsboom, A. Patra, S. S. Zade, Y. Sheynin, M. Li, L. J. W. Shimon and M. Bendikov, *Angew. Chem., Int. Ed.*, 2009, **48**, 5443.
24 M. Turbiez, P. Freère, M. Allain, N. Gallego-Planas and J. Roncali, *Macromolecules*, 2005, **38**, 6806.
25 Y. Liu, C. Di, C. Du, Y. Liu, K. Lu, W. Qiu and G. Yu, *Chem. – Eur. J.*, 2010, **16**, 2231.
26 X. C. Li, H. Sirringhaus, F. Garnier, A. B. Holmes, S. C. Moratti, N. Feeder, W. Clegg, S. J. Teat and R. H. Friend, *J. Am. Chem. Soc.*, 1998, **120**, 2206.

27 S. Ahn, K. Yabumoto, Y. Jeong and K. Akagi, *Polym. Chem.*, 2014, **5**, 6977.
28 T. T. Ong, S. C. Ng and H. S. O. Chan, *Polymer*, 2003, **44**, 5597.
29 B. Dong, Y. Xing, J. Xu, L. Zheng, J. Hou and F. Zhao, *Electrochim. Acta*, 2008, **53**, 5745.
30 M. Heeney, W. Zhang, D. J. Crouch, M. L. Chabinyc, S. Gordeyev, R. Hamilton, S. J. Higgins, I. McCulloch, P. J. Skabara, D. Sparrowea and S. Tierneya, *Chem. Commun.*, 2007, 5061.
31 A. Patra and M. Bendikov, *J. Mater. Chem.*, 2010, **20**, 422.
32 W. T. Neo, L. M. Loo, J. Song, X. Wang, C. M. Cho, H. S. O. Chan, Y. Zonga and J. Xu, *Polym. Chem.*, 2013, **4**, 4663.
33 S. Kaur, N. J. Findlay, A. L. Kanibolotsky, S. E. T. Elmasly, P. J. Skabara, R. Berridge, C. Wilsonc and S. J. Coles, *Polym. Chem.*, 2012, **3**, 2277.
34 O. V. Dolomanov, L. J. Bourhis, R. J. Gildea, J. A. K. Howard and H. Puschmann, OLEX2:a complete structure solution, refinement and analysis program, *J. Appl. Crystallogr.*, 2009, **42**, 339–341.
35 L. Palatinus and G. Chapuis, *J. Appl. Crystallogr.*, 2007, **40**, 786–790.
36 SHELXL, G. M. Sheldrick, *Acta Crystallogr., Sect. A: Found. Crystallogr.*, 2008, **A64**, 112–122.
37 M. J. Frisch, G. W. Trucks, H. B. Schlegel, G. E. Scuseria, M. A. Robb, J. R. Cheeseman, G. Scalmani, V. Barone, B. Mennucci, G. A. Petersson, H. Nakatsuji, M. Caricato, X. Li, H. P. Hratchian, A. F. Izmaylov, J. Bloino, G. Zheng, J. L. Sonnenberg, M. Hada, M. Ehara, K. Toyota, R. Fukuda, J. Hasegawa, M. Ishida, T. Nakajima, Y. Honda, O. Kitao, H. Nakai, T. Vreven, J. A. Montgomery Jr., J. E. Peralta, F. Ogliaro, M. Bearpark, J. J. Heyd, E. Brothers, K. N. Kudin, V. N. Staroverov, R. Kobayashi, J. Normand, K. Raghavachari, A. Rendell, J. C. Burant, S. S. Iyengar, J. Tomasi, M. Cossi, N. Rega, J. M. Millam, M. Klene, J. E. Knox, J. B. Cross, V. Bakken, C. Adamo, J. Jaramillo, R. Gomperts, R. E. Stratmann, O. Yazyev, A. J. Austin, R. Cammi, C. Pomelli, J. W. Ochterski, R. L. Martin, K. Morokuma, V. G. Zakrzewski, G. A. Voth, P. Salvador, J. J. Dannenberg, S. Dapprich, A. D. Daniels, O. Farkas, J. B. Foresman, J. V. Ortiz, J. Cioslowski and D. J. Fox, *Gaussian 09, Revision E.01*, Gaussian Inc., Wallingford CT, 2009.